Journal of Mammary Gland Biology and Neoplasia (2019) 24:39–45
https://doi.org/10.1007/s10911-018-9412-4

A Transgenic MMTV-Flippase Mouse Line for Molecular Engineering in Mammary Gland and Breast Cancer Mouse Models

Fabiana Lüönd[1] · Ruben Bill[1] · Andrea Vettiger[1,2] · Heide Oller[3] · Pawel Pelczar[3] · Gerhard Christofori[1]

Received: 6 June 2018 / Accepted: 4 September 2018 / Published online: 12 September 2018
© Springer Science+Business Media, LLC, part of Springer Nature 2018

Abstract

Genetically engineered mouse models have become an indispensable tool for breast cancer research. Combination of multiple site-specific recombination systems such as Cre/*loxP* and Flippase (Flp)/*Frt* allows for engineering of sophisticated, multi-layered conditional mouse models. Here, we report the generation and characterization of a novel transgenic mouse line expressing a mouse codon-optimized Flp under the control of the mouse mammary tumor virus (MMTV) promoter. These mice show robust Flp-mediated recombination in luminal mammary gland and breast cancer cells but no Flp activity in non-mammary tissues, with the exception of limited activity in salivary glands. These mice provide a unique tool for studying mammary gland biology and carcinogenesis in mice.

Keywords Breast cancer · Flippase · Lineage tracing · Mammary gland · MMTV promoter · Transgenic mice

Introduction

Despite major advances in understanding the mechanisms of malignant carcinogenesis, breast cancer is still a leading cause of cancer-related death in women worldwide. In the past decades, genetically engineered mouse models have contributed significantly towards understanding breast cancer development and progression. These include amongst others the widely used MMTV-driven transgenic mouse models, such as MMTV-PyMT or MMTV-Neu, as well as conditional models based on the knockout of tumor-suppressor genes, such as *Brca1*, *p53,* and *Cdh1* [1]. Recently, genetic lineage tracing approaches using conditional fluorescent reporters for the visualization of cell populations of interest have contributed towards our understanding of the origin of breast cancer [2–4], breast cancer stem cells [5], metastatic dissemination [6, 7] and chemoresistance [8].

Site-specific recombination systems such as Cre/*loxP* and Flp/*Frt* are powerful tools for the genetic manipulation of somatic cells in vivo. Briefly, these systems consist of a DNA recombinase and its unique short DNA target sequences. Cre recombinase of bacteriophage P1 recognizes and acts on 34 base pair *loxP* sites, while Flp recombinase of *Saccharomyces cerevisiae* specifically recombines 47 base pair *Frt* sites. Consequently, DNA sequences flanked by two *loxP* or *Frt* sites will be deleted upon Cre and Flp-mediated recombination, respectively, if the recognition sites are oriented in the same direction. In case the recognition sites are oriented in opposite directions, the flanked DNA sequence will be inverted. Although in murine models Cre has been initially found more efficient in catalyzing recombination than Flp, temperature-optimized version of Flp (Flpe) and mouse codon-optimized variants of Flpe (Flpo) are now almost as efficient as Cre [9–11].

✉ Gerhard Christofori
gerhard.christofori@unibas.ch

Fabiana Lüönd
fabiana.lueoend@unibas.ch

Ruben Bill
rubenmichael.bill@insel.ch

Andrea Vettiger
a.vettiger@unibas.ch

Heide Oller
heide.oller@unibas.ch

Pawel Pelczar
pawel.pelczar@unibas.ch

[1] Department of Biomedicine, University of Basel, Mattenstrasse 28, 4058 Basel, Switzerland

[2] Present address: Focal Area Infection Biology, Biozentrum University of Basel, Klingelbergstrasse 50/70, 4056 Basel, Switzerland

[3] Center for Transgenic Models, University of Basel, Mattenstrasse 22, 4058 Basel, Switzerland

To date, conditional breast cancer mouse models and genetic lineage tracing approaches most commonly rely on the widely used Cre/*loxP* system. In these models, Cre recombinase mediates excision of DNA to e.g. delete tumor suppressor genes or to remove a STOP cassette that prevents the expression of a fluorescent reporter or an activated oncogene. The choice of the promoter driving Cre expression is essential, as it determines the cell-lineage to be targeted in the mouse.

More recently, different site-specific recombination systems such as Cre/*loxP* and/or Flp/*Frt* or Dre/*Rox* have been combined in order to generate increasingly sophisticated model systems which combine the activation or inactivation of specific genes in a temporal and spatial manner [12–16]. Such dual recombinase-mediated approaches potentially allow to simultaneously target different cell-lineages, such as tumor and stromal cells or to modulate gene expression in the same cell-lineage in a sequential manner. The latter allows for the time-dependent introduction of mutations in tumor cells, for example by using inducible recombinases such as $CreER^{T2}$, or for the specific targeting of distinct tumor cell subpopulations in an individual tumor. Thus, the generation of novel Flp-driver lines and *Frt*-flanked alleles is required in order to establish "next-generation" dual recombinase-mediated mouse models for studying the tumor microenvironment, tumor progression and tumor heterogeneity in breast cancer. Here, we have generated a novel mouse line expressing a mouse codon-optimized Flp (Flpo) under the control of the MMTV promoter for the specific genetic manipulation of mammary gland epithelial cells and, in combination with adequate oncogene and/or tumor suppressor gene manipulations, in breast cancer cells.

Results and Discussion

In order to express the Flp recombinase in mammary gland epithelial cells, we placed the mouse codon-optimized *Flp* (*Flpo*) under the control of the MMTV promoter. Transgenic mice were generated by pronuclear microinjection. 17 founder animals were obtained, of which ten showed germline transmission.

To analyze Flpo activity in normal mammary gland epithelial cells, the founder lines were crossed with the RC::FrePe reporter strain [17, 18] (Fig. 1a). Briefly, this dual recombinase-responsive reporter allele encodes for mCherry and GFP whose expression can be controlled by Flp and Cre activity in a sequential manner. Since transcription of mCherry is prevented by a *Frt*-flanked STOP site, Flp-mediated recombination leads to mCherry expression. Upon fluorescence microscopy analysis of mCherry expression in mammary gland epithelial cells, two founder lines (9 and 11) with high Flpo activity were identified (Fig. 1b and c). Further analysis revealed that in animals of line 9 Flpo activity was restricted to cytokeratin 8/18 (CK-8/18)-positive luminal mammary gland cells, while Flpo was found active in both luminal and cytokeratin 14 (CK-14)-positive myoepithelial cells in mice of line 11 (Fig. 1b). Besides the mammary gland epithelium, also the pulmonary- and most notably the salivary gland epithelium are sites of MMTV promoter activity, which poses a risk of unwanted off-target effects. Interestingly, we did not detect any recombination in the lung and only very limited recombination in the salivary gland of line 9. However, we observed considerable Flpo activity in the lung and very strong activity in the salivary gland of line 11 (Fig. 1c). Consistent with this, Flpo expression levels were overall higher in animals of line 11 with particularly strong expression in salivary glands. Although we did not observe Flpo-mediated recombination in pulmonary epithelium of line 9, Flpo expression was detected by quantitative RT-PCR and, thus, low Flpo activity in the lung cannot be fully excluded (Fig. 1d).

The MMTV-PyMT transgenic mouse model is one of the most widely used models of metastatic breast cancer [19]. To generate mice developing tumors of the mammary glands, we crossed MMTV-Flpo/RC::FrePe double-transgenic mice with the MMTV-PyMT strain (Fig. 2a). Primary tumors and lung metastasis of both Flpo founder lines showed strong mCherry expression (Fig. 2b). Immunofluorescence staining for the stromal cell marker PDGFRβ and for the epithelial cell marker E-cadherin confirmed that Flpo activity of both mouse lines is specific to cancer cells. No leakiness of Flpo expression was observed in stromal cells (Fig. 2c).

Thus, both our MMTV-Flpo transgenic founder lines show high recombination efficiency in mammary gland epithelial cells and cancer cells in the MMTV-PyMT mouse model. However, Flpo activity of line 9 is spatially more restricted compared to line 11 and hence at lower risk for off-target effects. We therefore continued employing line 9 for further experimentation.

When breeding both male and female transgenic mice in strictly heterozygous matings we observed stable transgene transmission according to Mendelian inheritance. Follow-up analysis after at least four additional generations of breeding confirmed robust Flpo activity throughout the mammary glands (Fig. 3a). Overall, approximately 64% of luminal mammary gland epithelial cells showed mCherry expression in later generation MMTV-Flpo/RC::FrePe mice. There was no significant difference in recombination efficiencies at second and sixth filial generations ($65.20 \pm 1.22\%$ at F_2; $64.04 \pm 4.38\%$ at F_6). Similarly, approximately $67.45 \pm 4.71\%$, of cancer cells in PyMT driven breast tumors showed mCherry expression (Fig. 3b and c).

In the various MMTV-driven transgenic strains generated in the past years, differences in the onset of transgene expression have been observed. We hence performed time course

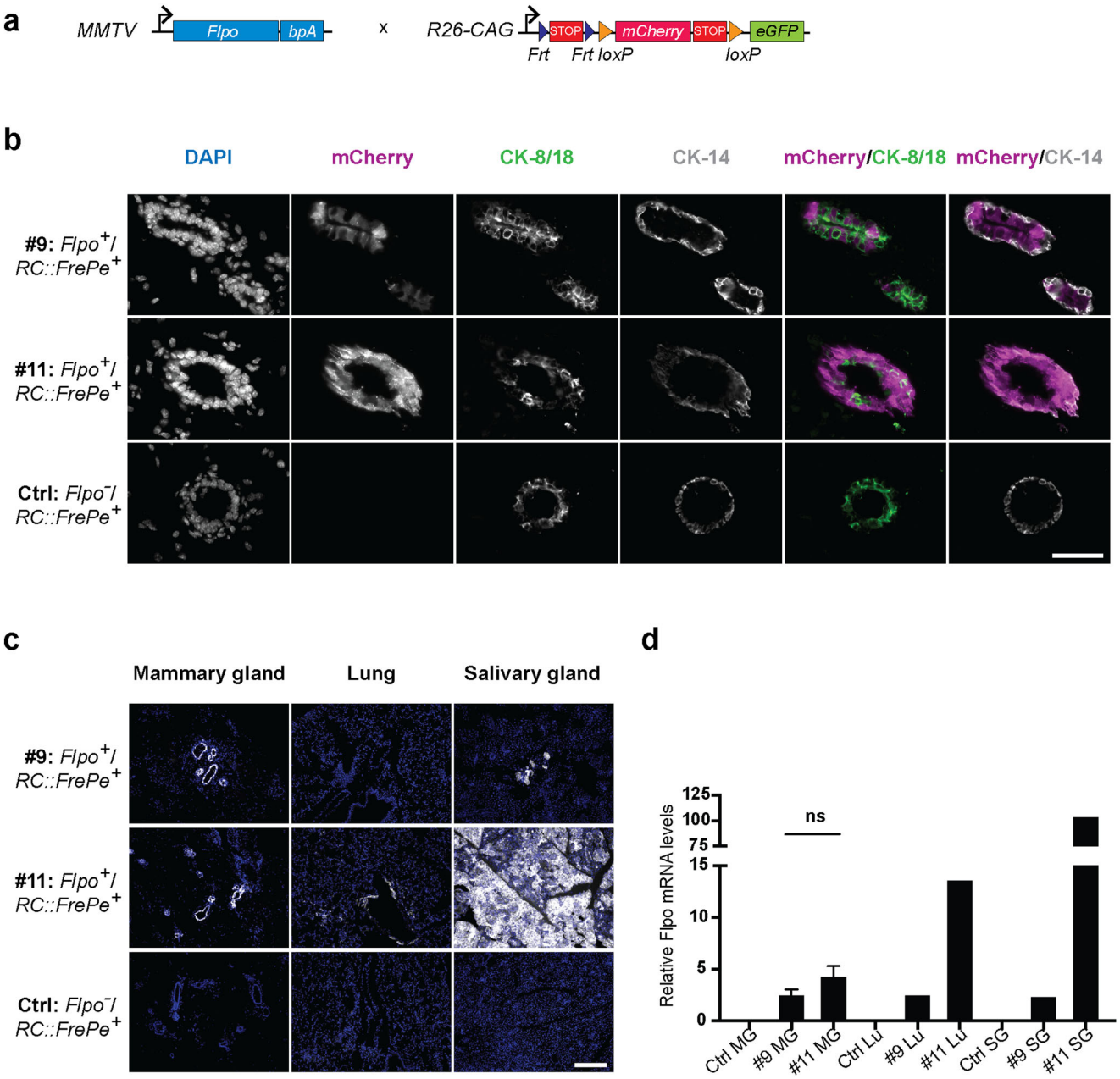

Fig. 1 Flpo activity in the mammary gland, lung and salivary gland. **a** Strategy for genetic lineage tracing of Flpo activity. Combination of *MMTV-Flpo* (left) and *RC::FrePe* (right) leads to stable mCherry expression in Flpo-expressing cells. **b** Co-staining of mammary glands with the luminal epithelial cell marker CK-8/18 (green) and myoepithelial cell marker CK-14 (grey). mCherry: magenta. Scale bar, 50μm. **c** Analysis of mCherry expression in mammary glands, lungs and salivary glands of adult female mice of MMTV-Flpo lines 9 and 11. mCherry: grey, DAPI: blue. Scale bar, 200μm. **d** Analysis of Flpo expression by quantitative RT-PCR in mammary glands (MG), lungs (Lu) and salivary glands (SG) of adult female mice of MMTV-Flpo lines 9 and 11. Mean and SEM of $n = 5$ mice are shown for mammary glands. Salivary gland and lung tissue of $n = 5$ mice were pooled prior to RNA extraction. Flpo expression levels were normalized to Gapdh. *P* value, 0.166; unpaired, two-tailed t-test

analysis to investigate the onset of Flpo expression in the mammary glands of MMTV-Flpo line 9. Flpo expression levels of four-week-old females were comparable to expression in eight-week-old females and low levels of Flpo expression could be detected already in two-week-old mice (Fig. 3d). Consistent with this, we observed mCherry expression in mammary glands of two and four-week-old mice indicating Flpo is active in mammary glands of mice as young as two weeks old (Fig. 3e and f).

In summary, we have generated and characterized a novel mouse line expressing Flpo under the control of the MMTV promoter. This line shows robust Flpo activity in luminal mammary gland epithelial cells. Since Flpo is already expressed in the developing mammary glands of prepubertal

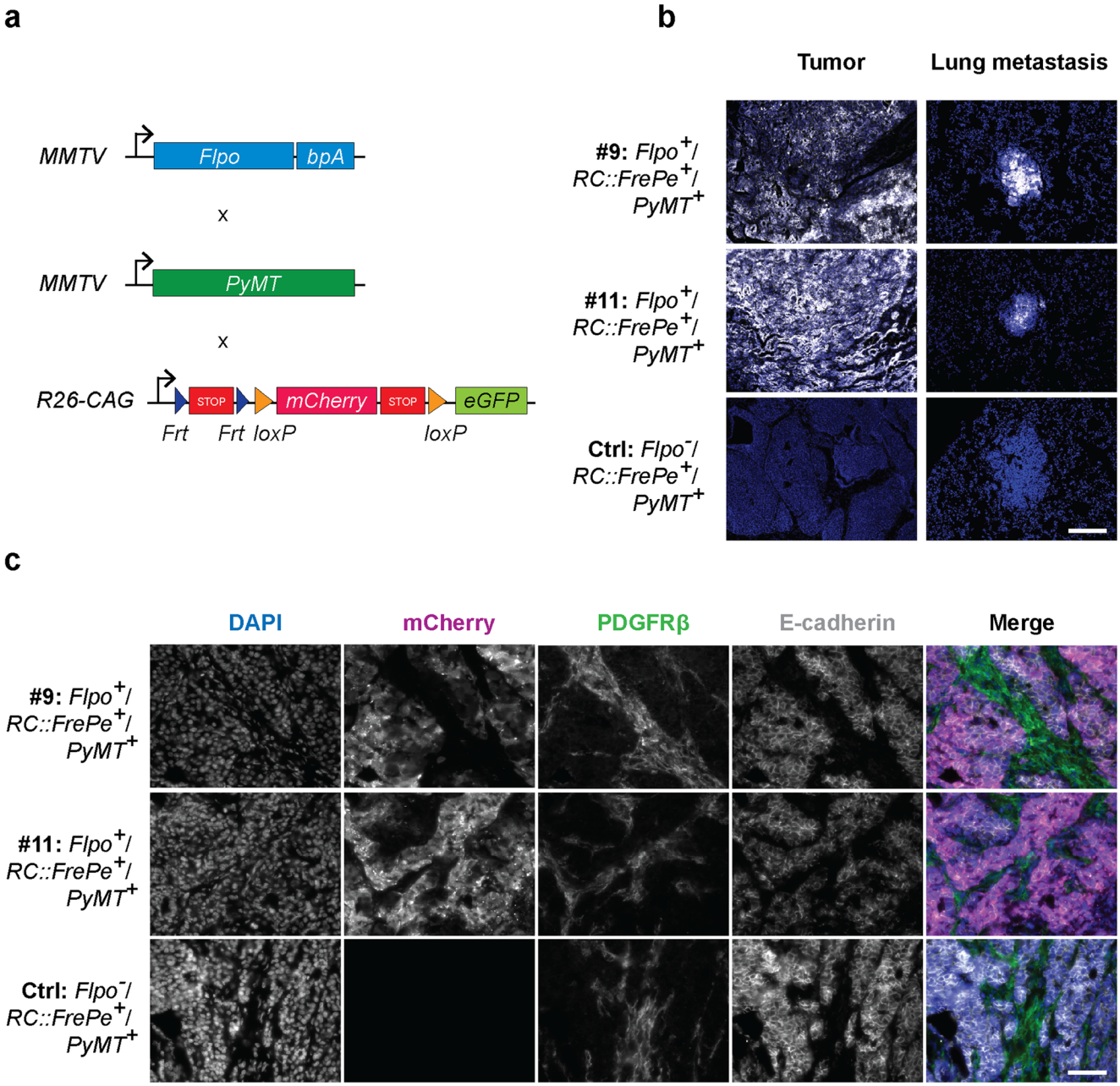

Fig. 2 Flpo activity in breast cancer cells of MMTV-PyMT mice. **a** Strategy for genetic lineage tracing of Flpo activity in breast cancer cells of MMTV-PyMT transgenic mice. Combination of *MMTV-Flpo* (top), *MMTV-PyMT* (middle) and *RC::FrePe* (bottom) leads to stable mCherry expression in Flpo-expressing tumor cells. **b** Analysis of mCherry expression in primary tumors and lung metastasis of MMTV-Flpo mouse lines 9 and 11. mCherry: grey, DAPI: blue. Scale bar, 200μm. **c** Co-staining of primary tumors for the stromal cell marker PDGFRβ (green) and the epithelial cell marker E-cadherin (grey). mCherry: magenta, DAPI: blue. Scale bar, 50μm

mice, the mouse line may also be useful for research focusing on pubertal mammary gland development. Furthermore, the mouse line may be crossed to strains harboring *Frt*-flanked tumor suppressor genes, such as $p53^{Frt/Frt}$ or an activated version of oncogenes [20] for the generation of novel conditional breast cancer mouse models. Importantly, our new mouse line offers new opportunities for genetic lineage tracing in breast cancer, particularly in the widely used MMTV-driven mouse models. For example, combination of MMTV-Flpo, RC::FrePe and a Cre driver line of choice may be readily used to visualize cancer cell subpopulations of interest, for example in MMTV-PyMT-driven tumors. With novel *Frt*-flanked conditional alleles and increasingly complex site-specific recombinase-responsive reporter alleles becoming available, our mouse line has the potential to become a versatile tool for genetic manipulation and lineage tracing in the murine mammary gland and in mammary gland cancer.

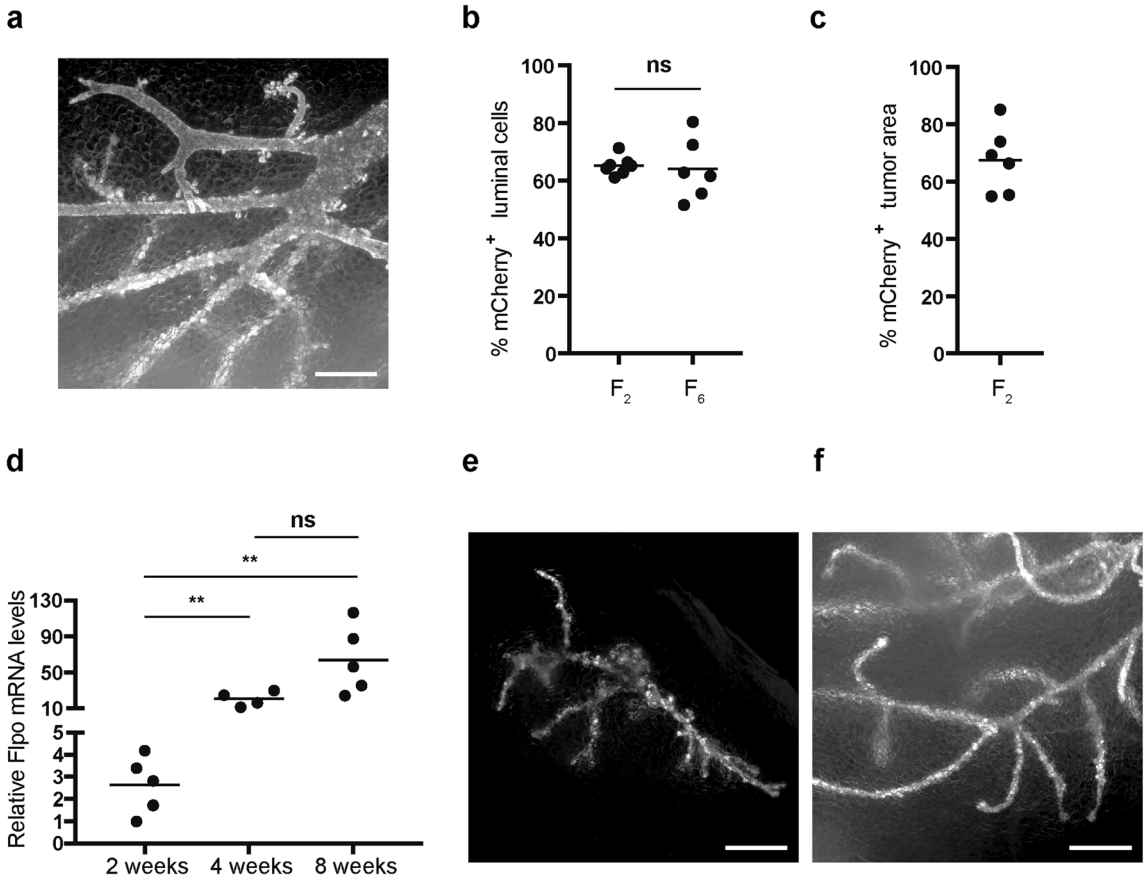

Fig. 3 Efficiency and onset of Flpo activity in the MMTV-Flpo mouse line 9. **a** Mammary glands of *MMTV-Flpo*$^{+}$*/RC::FrePe*$^{+}$ adult (8-week-old) female mice (whole mounted tissue). mCherry: grey. Scale bar, 500μm. **b** Flpo recombination efficiency in mammary glands of 8-week-old mice at filial generations F_2 and F_6. Means of $n = 7$ (F_2) and $n = 6$ (F_6) individual mice are shown. Five imaging fields (63× magnification) were analyzed per mouse. *P* value, 0.7902; unpaired, two-tailed t-test. **c** Flpo recombination efficiency in breast tumors of *MMTV-PyMT*$^{+}$*/MMTV-Flpo*$^{+}$*/RC::FrePe*$^{+}$ *triple-transgenic mice*. The mean of $n = 6$ individual mice are shown. Two tumor sections were analyzed per mouse. **d** Analysis of Flpo expression by quantitative RT-PCR in mammary glands of 2, 4 and 8-week-old female mice. Means of $n = 5$ (2 weeks), $n = 4$ (4 weeks) and $n = 5$ (8 weeks) mice are shown. Flpo expression levels were normalized to Gapdh. *P* values: 0.0018 (2 vs 4 weeks), 0.0068 (2 vs 8 weeks), 0.0620 (4 vs 8 weeks). **e**, **f** Mammary glands of *MMTV-Flpo*$^{+}$*/RC::FrePe*$^{+}$ 2-week-old (**e**) and 4-week-old (**f**) female mice (whole mounted tissue). mCherry: grey. Scale bar, 500μm

Materials and Methods

Animals

Mouse colonies were kept at the animal facility of the Department of Biomedicine, University of Basel, Switzerland. All animal experiments were carried out in accordance with the guidelines of the Swiss Federal Veterinary Office (SFVO) and the Cantonal Veterinary Office of Basel-Stadt (Licenses 1878, 1023G1). MMTV-PyMT (FVB/N) mice were a kind gift of N. Hynes (FMI, Basel, Switzerland). RC::FrePe mice (B6;129S6-Gt(ROSA)26Sortm8(CAG-mCherry,-EGFP)Dym/J) were a kind gift of S. Dymecki (Department of Genetics, Harvard Medical School, Boston, Massachusetts). The mice were crossed six to seven generations into the FVB/N background and then used for the experiments. All experiments were performed on female mice. For analysis of the mammary gland, mice were sacrificed at eight weeks, four weeks or two weeks of age. Tumor bearing mice were sacrificed before a tumor volume of 1500mm^3 was reached, usually at 12–13 weeks of age.

Construction of the Flp Expression Vector

The mouse codon-optimized Flp (*Flpo*) gene was placed under the control of the *MMTV LTR* promoter. The pPGKFlpobpA plasmid was a kind gift from Philippe Soriano (Addgene plasmid # 13793). The vector containing the *MMTV-LTR* and *BGHpA* was a kind gift from Kari Alitalo. The *Flpo* fragment was PCR amplified from the pPGKFlpobpA plasmid and inserted into the vector as an XhoI fragment.

Generation and Genotyping of Transgenic Mice

The *MMTV-Flpo-BGHpA* was released from the construct as a HindIII-NdeI fragment and purified using the QIAEX II Gel Extraction Kit (Qiagen) according to the manufacturer's instructions. The fragment was then microinjected into the pronuclei of FVB/N zygotes and the embryos were transferred into pseudopregnant CD1 females at the Center for Transgenic Models (University of Basel, Switzerland). Transgenic founders were identified by PCR using primers 5'-CCA AGG TGC TGG TGC GGC AGT TCG TG-3′ and 3`-GAT CTC CCA GAT GCT CTC GCC CTC GGA C-5 resulting in a 436 bp PCR product in transgenic mice. The established MMTV-Flpo line (FVB/N-Tg(MMTV-Flpo)9Gcr) was kept heterozygous and in a pure FVB/N background. Transgenic progeny was identified by PCR as described above or alternatively using primer pair 5′-TGA GCT TCG ACA TCG TGA AC-3′ and 3'-TCA GCA TCT TCT TGC TGT GG-3′ generating a 231 bp product.

Immunofluorescent Staining

Tissues were fixed in 4% PFA for two hours and incubated in 20% sucrose overnight at 4 °C. Tissues were then embedded in Tissue-Tek O.C.T compound (Sakura), snap-frozen and stored at −80 °C. 7 μm thick tissue sections were cut, dried for 30 min, rehydrated in PBS, permeabilized with 0.2% Triton X-100 in PBS for 20 min and blocked with 5% normal goat serum (NGS; Sigma-Aldrich; G6767) in PBS for one hour. Next, sections were incubated with primary antibody overnight at 4 °C followed by 1 h incubation with secondary antibody at room temperature. All antibodies were diluted in 5% NGS in PBS. The following primary antibodies were used: guinea pig-anti-CK8/18 (Fitzgerald Industries; 20R-CP004; 1:50), rabbit-anti-CK14 (Thermo Scientific; RB-9020; 1:50), rat-anti-E-cadherin (clone ECCD-2; Invitrogen; 13–1900; 1:400), rabbit-anti-PDGFRβ (clone Y92; abcam; ab32570; 1:100). Secondary antibodies directed against the species of the primary antibody were coupled to Alexa 488 or Alexa 647 (Invitrogen; 1:400). Nuclei were stained with 4′,6-Diamidin-2-phenylindol (DAPI; Sigma-Aldrich; 1:5000) for 10 min at room temperature. The sections were mounted with Dako fluorescence mounting medium (Agilent). Images were acquired with a Leica DMI 4000 microscope and processed with ImageJ.

RNA Isolation and Quantitative RT-PCR

Total RNA was isolated using RNAeasy Mini Kit (Qiagen). On column DNA digestion using RNAse-Free DNase Set (Qiagen) was performed. Prior to isolation, tissue of thoracic and abdominal mammary glands was pooled for every individual mouse. Salivary gland and lung tissue of five mice was pooled. cDNA was synthesized using ImProm-II Reverse Transcriptase (Promega). Quantitative RT-PCR was performed on a StepOnePlus machine (Applied Biosystems) using Power-Up SYBR green (Applied Biosystems). Flpo expression levels were normalized to Gapdh. *Flpo*-specific primers 5′-ccgagaagatcctgaacagc-3′ (forward) and 5′-ggtacagggtcttggtcttgg-3′ (reverse) and *Gapdh*-specific primers 5′- agcttgtcatcaacgggaag-3′ and 5′-tttgatgttagtggggtctcg-3′ were used.

Mammary Gland Whole Mounts

Isolated mammary glands were mounted on a glass-slide and imaged with a Leica DMI 4000 microscope.

Quantification of Recombination Efficiency

For quantification of Flpo-mediated recombination efficiency in the mammary gland, the total numbers of cytokeratin 8/18 positive (luminal) cells and the number of mCherry expressing cytokeratin 8/18 positive cells were counted. Five imaging fields each of mammary glands (63× magnification) from a total of 7 (F_2) and 6 (F_6) mice were analyzed. For quantification of the levels of recombined cells in PyMT tumors, sections of two different tumors per mouse were analyzed. The whole tumor section was imaged with a Zeiss Axio Imager Scanning Microscope (10× magnification). The mCherry-positive area and total tumor areas (DAPI positive area) were determined by global thresholding (Otsu algorithm) using ImageJ. Six mice (F_2) were analyzed.

Statistical Analysis

Statistical analysis was performed using GraphPad Prism (GraphPad Software Inc.). Graphs display single measurement points and means or mean + SEM. Unpaired, two-tailed t-tests were performed.

Data Availability All data and materials are freely available to the research community. The newly generated transgenic mouse line is available by a Material Transfer Agreement.

Acknowledgments We thank P. Lorentz for support with microscopy and H. Antoniadis and U. Schmieder for technical support. We are grateful to S. Dymecki and N. Hynes for providing mice and P. Soriano and K. Alitalo for plasmids. R.B. was supported by a MD-PhD fellowship of the Swiss National Science Foundation and Swiss Cancer League. The work was supported by the Swiss National Science Foundation and the Swiss Cancer League.

Author's Contributions F.L. designed and performed the experiments, analysed the data and wrote the manuscript. R.B. conceived the idea and designed some of the experiments and analysed the data. A.V. performed some of the experiments. H.O. and P.P. performed the pronuclei microinjections. G.C. supervised the project, designed the experiments, analysed the data and wrote the manuscript.

Compliance with Ethical Standards

Conflicts of Interest The authors declare no financial and non-financial competing interests.

Ethical Approval All animal experiments were carried out in accordance with the guidelines of the Swiss Federal Veterinary Office (SFVO) and the Cantonal Veterinary Office of Basel-Stadt (license numbers 1878, 1023G1).

Informed Consent No individual person's data has been used in this project.

Abbreviations *MMTV,* Mouse mammary tumor virus; *Flp,* Flippase; *Flpo,* mouse codon usage-optimized Flp; *CK,* cytokeratin

References

1. Borowsky AD. Choosing a mouse model: experimental biology in context–the utility and limitations of mouse models of breast cancer. Cold Spring Harb Perspect Biol. 2011;3(9):a009670. https://doi.org/10.1101/cshperspect.a009670.
2. Van Keymeulen A, Lee MY, Ousset M, Brohee S, Rorive S, Giraddi RR, et al. Reactivation of multipotency by oncogenic PIK3CA induces breast tumour heterogeneity. Nature. 2015;525(7567):119–23. https://doi.org/10.1038/nature14665.
3. Koren S, Reavie L, Couto JP, De Silva D, Stadler MB, Roloff T, et al. PIK3CA(H1047R) induces multipotency and multi-lineage mammary tumours. Nature. 2015;525(7567):114–8. https://doi.org/10.1038/nature14669.
4. Blaas L, Pucci F, Messal HA, Andersson AB, Josue Ruiz E, Gerling M, et al. Lgr6 labels a rare population of mammary gland progenitor cells that are able to originate luminal mammary tumours. Nat Cell Biol. 2016;18(12):1346–56. https://doi.org/10.1038/ncb3434.
5. Zomer A, Ellenbroek SI, Ritsma L, Beerling E, Vrisekoop N, Van Rheenen J. Intravital imaging of cancer stem cell plasticity in mammary tumors. Stem Cells. 2013;31(3):602–6. https://doi.org/10.1002/stem.1296.
6. Beerling E, Seinstra D, de Wit E, Kester L, van der Velden D, Maynard C, et al. Plasticity between epithelial and mesenchymal states unlinks EMT from metastasis-enhancing stem cell capacity. Cell Rep. 2016;14(10):2281–8. https://doi.org/10.1016/j.celrep.2016.02.034.
7. Cheung KJ, Padmanaban V, Silvestri V, Schipper K, Cohen JD, Fairchild AN, et al. Polyclonal breast cancer metastases arise from collective dissemination of keratin 14-expressing tumor cell clusters. Proc Natl Acad Sci U S A. 2016;113(7):E854–63. https://doi.org/10.1073/pnas.1508541113.
8. Fischer KR, Durrans A, Lee S, Sheng J, Li F, Wong ST, et al. Epithelial-to-mesenchymal transition is not required for lung metastasis but contributes to chemoresistance. Nature. 2015;527(7579):472–6. https://doi.org/10.1038/nature15748.
9. Branda CS, Dymecki SM. Talking about a revolution: The impact of site-specific recombinases on genetic analyses in mice. Dev Cell. 2004;6(1):7–28.
10. Olorunniji FJ, Rosser SJ, Stark WM. Site-specific recombinases: molecular machines for the genetic revolution. Biochem J. 2016;473(6):673–84. https://doi.org/10.1042/BJ20151112.
11. Dymecki SM, Ray RS, Kim JC. Mapping cell fate and function using recombinase-based intersectional strategies. Methods Enzymol. 2010;477:183–213. https://doi.org/10.1016/S0076-6879(10)77011-7.
12. Schonhuber N, Seidler B, Schuck K, Veltkamp C, Schachtler C, Zukowska M, et al. A next-generation dual-recombinase system for time- and host-specific targeting of pancreatic cancer. Nat Med. 2014;20(11):1340–7. https://doi.org/10.1038/nm.3646.
13. Shai A, Dankort D, Juan J, Green S, McMahon M. TP53 silencing bypasses growth arrest of BRAFV600E-induced lung tumor cells in a two-switch model of lung tumorigenesis. Cancer Res. 2015;75(15):3167–80. https://doi.org/10.1158/0008-5472.CAN-14-3701.
14. Young NP, Crowley D, Jacks T. Uncoupling cancer mutations reveals critical timing of p53 loss in sarcomagenesis. Cancer Res. 2011;71(11):4040–7. https://doi.org/10.1158/0008-5472.CAN-10-4563.
15. Moding EJ, Lee CL, Castle KD, Oh P, Mao L, Zha S, et al. Atm deletion with dual recombinase technology preferentially radiosensitizes tumor endothelium. J Clin Invest. 2014;124(8):3325–38. https://doi.org/10.1172/JCI73932.
16. He L, Li Y, Li Y, Pu W, Huang X, Tian X, et al. Enhancing the precision of genetic lineage tracing using dual recombinases. Nat Med. 2017;23(12):1488–98. https://doi.org/10.1038/nm.4437.
17. Bang SJ, Jensen P, Dymecki SM, Commons KG. Projections and interconnections of genetically defined serotonin neurons in mice. Eur J Neurosci. 2012;35(1):85–96. https://doi.org/10.1111/j.1460-9568.2011.07936.x.
18. Engleka KA, Manderfield LJ, Brust RD, Li L, Cohen A, Dymecki SM, et al. Islet1 derivatives in the heart are of both neural crest and second heart field origin. Circ Res. 2012;110(7):922–6. https://doi.org/10.1161/CIRCRESAHA.112.266510.
19. Guy CT, Cardiff RD, Muller WJ. Induction of mammary tumors by expression of polyomavirus middle T oncogene: a transgenic mouse model for metastatic disease. Mol Cell Biol. 1992;12(3):954–61.
20. Lee CL, Moding EJ, Huang X, Li Y, Woodlief LZ, Rodrigues RC, et al. Generation of primary tumors with Flp recombinase in FRT-flanked p53 mice. Dis Model Mech. 2012;5(3):397–402. https://doi.org/10.1242/dmm.009084.